

A Mathematical Model of Bipolar Radiofrequency-Induced Thermofusion*

J. Wagenpfeil¹, B. Nold², K. Fischer², A. Neugebauer²,
R. Rothmund³, B. Krämer³, S. Brucker³, J. Mischinger³, C. Schwentner³,
M. Schenk³, D. Wallwiener³, A. Stenzl³, M. Enderle², O. Sawodny¹, and M. Ederer¹

Abstract—Bipolar radiofrequency-induced thermofusion has become a widely accepted method successfully used in open and particularly in minimally-invasive surgery for the sealing of blood vessels and tissue of up to several millimeters diameter. Despite its wide-spread application, the thermofusion process itself is not well understood on a quantitative and dynamic level, and manufacturers largely rely on trial-and-error methods to improve existing instruments. To predict the effect of alternative generator control strategies and to allow for a more systematic approach to improve thermofusion instruments, a mathematical model of the thermofusion process is developed. The system equations describe the spatial and temporal evolution of the tissue temperature due to Joule heating and heat transfer, and the loss of tissue water due to vaporization. The resulting effects on the tissue properties, most importantly the electrical resistivity, heat capacity and thermal conductivity, are considered as well. Experimental results indicate that the extent of the lateral thermal damage is directly affected by Joule heating of the lateral tissue. The experimental findings are supported by simulation results using the proposed mathematical model of thermofusion.

I. INTRODUCTION

Radiofrequency-induced bipolar vessel sealing, also known as thermofusion, is an electrosurgical procedure for the vascular occlusion of blood vessels of up to 6 mm diameter [1]. A bipolar vessel sealing system usually consists of a high-frequency alternating current generator and a thermofusion instrument which is typically designed as forceps with electrodes on the jaws of the instrument. During surgery, the blood vessel to be sealed is firmly grasped between the jaws (see Fig. 1) and an alternating current is applied directly through the grasped tissue. Joule heating due to the electrical resistivity of the tissue results in the denaturation of collagen and other proteins. Under pressure, the uncoiled peptide chains form new coherent structures, effectively fusing the two vessel walls together, and create a reliable occlusion of the blood vessel.

Thermofusion instruments are used in many surgical procedures for the safe and reliable sealing of larger blood vessels, as well as for the hemostasis of smaller vessels

*This work was supported by ERBE Elektromedizin GmbH, the German federal state Baden-Württemberg and the Universities of Tübingen and Stuttgart within the Industry on Campus projects of the Inter-University Center for Medical Technology Stuttgart-Tübingen (IZST).

¹Institute for System Dynamics, University of Stuttgart, 70569 Stuttgart, Germany, contact: wagenpfeil@isys.uni-stuttgart.de

²ERBE Elektromedizin GmbH, Waldhörnlestraße 17, 72072 Tübingen, Germany

³University Hospital Tübingen, Geissweg 3, 72076 Tübingen, Germany

for the nearly bloodless preparation of tissue structures, both in open and minimally-invasive surgery. Despite their widespread use, most modern bipolar vessel sealing systems are still the result of a highly empirical development process. Key parameters of the instruments like form, size, or surface structure of the jaws have been iteratively improved based on the experience with earlier variants and the results of many trial-and-error experimental studies. An important aspect, besides the quality of the sealing, is the thermal damaging of the lateral tissue. This is especially the case when using thermofusion instruments to prepare tissue close to thermosensitive structures that must not be damaged, like e.g. nerves or the ureters. Both, the sealing quality and the extent of the thermal damage are affected by a large number of parameters. The relation of the parameters among each other and their specific effect on the sealing quality and thermal damage is not fully understood.

In the field of electrosurgery, only few mathematical modeling approaches have been reported in the literature, many of which focus on monopolar applications like radiofrequency tissue ablation. All models use a finite element (FE) modeling approach for a coupled simulation of the electric field and the temperature of the tissue. Dodde et al. [2] developed a thermo-electric model to study the temperature distribution assuming different electrode geometries. This model was extended by Chen et al. [3] to account for changes in the specific heat capacity, electrical resistance and water contents of the tissue during the thermofusion process. Gonzalez-Suarez et al. [4] presented a FE model for a bipolar instrument with internally cooled electrodes. Unfortunately, the high level of detail of FE models results in a very large number of state variables and hence requires much computational time. Standard FE modeling tools typically are not able to simulate effects like evaporation and the resulting loss of mass and change of properties directly. For a systematic analysis of the thermofusion process, the mathematical model must reproduce the relevant dynamics while being as concise as possible.

In this work, a dynamical model of bipolar thermofusion is proposed. The system equations describe the spatial and temporal evolution of the tissue temperature due to Joule heating and heat transfer, and the loss of tissue water due to vaporization and the resulting effect on the tissue properties, most importantly electrical resistivity, heat capacity and thermal conductivity. This model may be used for a



Fig. 1. Application of the ERBE BiClamp[®] 201 C to occlude the vasculature during vaginal hysterectomy. Image courtesy of ERBE GmbH.

detailed analysis of the influence of different parameters and thus help to achieve a better understanding of the vessel sealing process. Building on that, the model may help to systematically improve existing thermofusion instruments and to develop more effective control strategies, both with the goal of optimizing the vessel sealing quality while at the same time minimizing the lateral damage.

II. MODELING

Consider a single blood vessel, held between the two forceps of a thermofusion instrument as shown in Fig. 2. It is assumed that both the instrument and the blood vessel are symmetric with respect to the x - y -plane. Let $2w_T$ and $2w_M$ be the width of the tissue and the jaws, respectively, and let $w_L = w_T - w_M$ denote the width of the lateral tissue. To reduce the number of state variables, only the right half of the system is considered, i.e. $z \in (0, w_T)$. In the following it is assumed, that the tissue can be considered as a homogenous ideal composite of water and dry tissue matter. Let the state variables be the temperature T , the pressure p , and the mass of water and dry tissue matter, m_W and m_D , respectively. Then, any extensive property $\Phi(T, p, m_W, m_D)$ is given by

$$\Phi(T, p, m_W, m_D) = m_W \phi_W(T, p) + m_D \phi_D(T, p), \quad (1)$$

where ϕ_W and ϕ_D are the corresponding mass-specific properties of water and dry tissue matter, respectively. It is assumed that the tissue is homogenous across its cross-section, which means that the temperature $T = T(t, z)$, and the masses $m_i = m_i(t, z)$ depend only on the lateral position z and the time t . It is furthermore assumed that the pressure is constant, i.e. $p(t, z) = p_0$, and that the tissue is incompressible, i.e. the mass-specific volumes of water v_W and dry tissue v_D are constant.

A. Infinitesimal volume element

Consider an infinitesimal volume element of the tissue, as shown in Fig. 2, with infinitesimally small width dz . The volume of the volume element is given by $V(t, z) = A(t, z)dz$, where $A(t, z)$ is the cross sectional area of the tissue. Similarly, the mass of water and the mass of dry matter are given by $m_W = m'_W dz$ and $m_D = m'_D dz$, with m'_W and m'_D denoting the specific mass of water and dry matter, respectively. Note that the term *specific* refers to specific with respect to the width dz , if not stated otherwise.

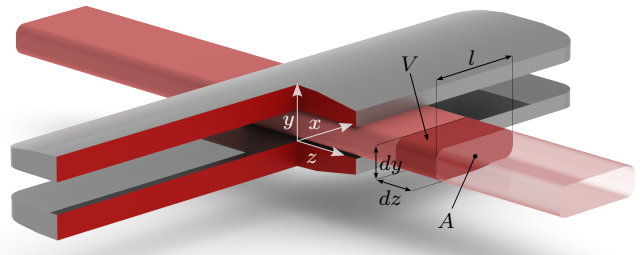


Fig. 2. Experimental setup of the thermofusion instrument and the vessel grasped between the electrodes.

B. Specific mass balance

Due to evaporation, the water contents of the tissue decreases during the sealing process, while the amount of dry matter remains unchanged. It is assumed that the vaporized tissue water immediately leaves the volume element into the environment. Let $j_{m, \text{vap}}$ be the specific evaporation rate, then the specific mass balances of water and dry tissue matter are given by

$$\dot{m}'_W(t, z) = -j_{m, \text{vap}}(t, z) \quad \text{and} \quad \dot{m}'_D(t, z) = 0, \quad (2)$$

respectively.

C. Tissue temperature

According to equation (1), the enthalpy of the volume element is given by

$$H(T, p, m_W, m_D) = m_W h_W(T, p) + m_D h_D(T, p), \quad (3)$$

where h_W and h_D are the mass-specific enthalpies of water and dry tissue matter, respectively. For constant pressure p_0 , the mass-specific enthalpy is given by

$$h(T, p_0) = c_p T + h_0, \quad (4)$$

where c_p is the mass-specific heat capacity, and h_0 is an arbitrary constant value. Differentiation with respect to time yields

$$\dot{H} = -J_{m, \text{vap}} h_W + \dot{T} \cdot (m_W c_{p, W} + m_D c_{p, D}), \quad (5)$$

with $J_{m, \text{vap}} = j_{m, \text{vap}} dz$.

The first law of thermodynamics in terms of the enthalpy is given by

$$\dot{H} = J_{Q, \text{ht}} + J_{Q, \text{ex}} + J_{Q, \text{el}} - J_{m, \text{vap}}(h_W + \Delta h_{\text{vap}, W}), \quad (6)$$

where $J_{Q, \text{ht}}$ is the heat flow into the volume element through heat transfer in z -direction, $J_{Q, \text{ex}}$ is the heat loss into the environment, $J_{Q, \text{el}}$ is the rate of heat generated by electric Joule heating within the volume element, and $J_{m, \text{vap}}(h_W + \Delta h_{\text{vap}, W})$ is the enthalpy of the vaporized tissue water leaving the volume element. Inserting equation (5) results in the differential equation for the tissue temperature

$$\dot{T} = \frac{J_{Q, \text{ht}} + J_{Q, \text{ex}} + J_{Q, \text{el}} - J_{m, \text{vap}} \Delta h_{\text{vap}, W}}{m_W c_{p, W} + m_D c_{p, D}}. \quad (7)$$

For the infinitesimal volume element under consideration, equation (7) becomes

$$\dot{T} = \frac{\dot{q}_{\text{ht}} + \dot{q}_{\text{ex}} + \dot{q}_{\text{el}} - j_{m, \text{vap}} \Delta h_{\text{vap}, W}}{m'_W c_{p, W} + m'_D c_{p, D}}, \quad (8)$$

where the \dot{q}_i denote the specific heat flows.

D. Specific evaporation rate

From the observation that the temperature does not exceed the boiling temperature of water, the maximum specific evaporation rate is derived from equation (8) by inserting $\dot{T} = 0$ on the left side:

$$\dot{j}_{m,\text{vap,max}} = \frac{1}{\Delta h_{\text{vap,w}}} (\dot{q}_{\text{ht}} + \dot{q}_{\text{ex}} + \dot{q}_{\text{el}}). \quad (9)$$

Assuming that there is no condensation, i.e. the evaporation rate is always non-negative, and that evaporation does not begin abruptly at 100°C , the specific evaporation rate can be modeled as

$$\dot{j}_{m,\text{vap}} = \max\left(0, e^{T-100^\circ\text{C}} \cdot \dot{j}_{m,\text{vap,max}}\right). \quad (10)$$

E. Specific heat transfer

Let λ denote the appropriate heat transfer coefficients. The specific heat flow into the environment \dot{q}_{ex} is modeled by

$$\dot{q}_{\text{ex}}(t, z) = -\lambda_{\text{ex}} (T(t, z) - T_{\text{ex}}). \quad (11)$$

The specific heat transfer \dot{q}_{ht} is modeled by Fourier's law

$$\dot{q}_{\text{ht}}(t, z) = \frac{\partial}{\partial z} \left(-\lambda(t, z) A(t, z) \frac{\partial T(t, z)}{\partial z} \right). \quad (12)$$

Thus, the temperature differential equation becomes a partial differential equation (PDE). The boundary conditions are

$$\dot{q}_{\text{ht}}(t, z) = 0 \Big|_{z=0}, \quad \text{and} \quad (13)$$

$$\dot{q}_{\text{ht}}(t, z) = -\lambda_{\text{bc}} (T(t, z) - T_{\text{ex}}) \Big|_{z=w_{\text{T}}}, \quad (14)$$

where equation (13) is given due to the assumed symmetry to $z = 0$, and equation (14) models the specific heat flow into the environment on the right boundary.

F. Joule heating

Assuming that the cross sectional area is rectangular, i.e. $A(t, z) = dy \cdot l(t, z)$, then the specific heat generated by the electric current passing through the infinitesimal volume element is given by

$$\dot{q}_{\text{el}}(t, z) = \frac{l(t, z)}{dy \cdot r(t, z)} U^2(t, z), \quad (15)$$

which models the specific electrical power of an ohmic resistor with uniform cross section, see e.g. [5]. Here, dy is the distance between the electrodes, i.e. the thickness of the tissue, $l(t, z)$ is the length of the tissue, and $r(t, z)$ is the specific electrical resistivity (see next section). The voltage $U(t, z)$ applied to the medial tissue is given by the voltage $U_{\text{E}}(t)$ impressed between the electrodes, and assumed to be constant over the spatial domain of the electrode, i.e.

$$U(t, z) = U_{\text{E}}(t) \quad \text{for } z \in [0, w_{\text{M}}]. \quad (16)$$

A preliminary evaluation of the surface temperatures of the lateral tissue during *ex vivo* vessel sealing experiments shows an increase that is too fast to be caused alone by heat transfer from the medial tissue. A possible explanation for

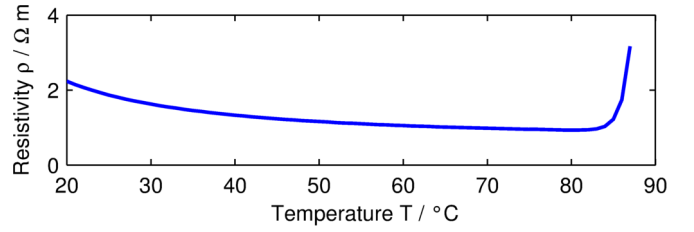


Fig. 3. Temperature dependent tissue resistivity as given by (18).

this effect is Joule heating within the lateral tissue near the edge of the electrodes. The electrical field is approximated by an analogous voltage, which is applied to the lateral tissue according to equation (15). The voltage $U(t, z)$ applied to the lateral tissue is assumed to equal the voltage impressed between the electrodes at the edge of the instrument and to decrease exponentially with the distance from the instrument, i.e.

$$U(t, z) = e^{\alpha(w_{\text{M}}-z)} \cdot U_{\text{E}}(t) \quad \text{for } z \in (w_{\text{M}}, w_{\text{T}}), \quad (17)$$

where $\alpha > 0$ is a tuning parameter that determines how far the simulated electrical field extends into the lateral tissue.

G. Tissue resistivity

For the electrical resistivity, the phenomenological model

$$r(t, z) = \left(c + \frac{b_1 T(t, z) - b_0}{T^{a_1}(t, z) + a_0} \right) + r_{\text{max}} \cdot e^{T(t, z) - T_{\text{vap}}} \quad (18)$$

was chosen to describe the resistivity as a function of the tissue temperature $T(t, z)$. The coefficients a_i , b_j , and c were fitted to measurement data and describe the tissue resistivity for temperatures well below vaporization temperature. The exponential term, with $r_{\text{max}} \gg 1$, describes the dominating resistivity increase that is observed for higher temperatures. The resulting resistivity is shown in Fig. 3 for the relevant temperature range.

H. Other parameters

Parameter values reported in the literature, such as the mass-specific heat capacities c_p , heat transfer coefficients λ or electric resistance, were set to the reported values, see e.g. [6]. The remaining unknown parameters were fitted using a single set of measurement data and validated using the remaining measurement data sets.

III. RESULTS

A. Experimental data

Data was provided by ERBE Elektromedizin GmbH in the form of the electric currents and voltages measured during *ex vivo* vessel sealing experiments. Renal arteries with a diameter of about 6.5 mm, taken from domestic pigs, were sealed using the BiClamp[®] 201 T thermofusion instrument. The AC generator used the proprietary voltage controlled BiClamp mode to impose a series of rectangular voltage pulses, see Fig. 4 (red dotted line). The resulting characteristic course of the voltage and current is shown Fig. 4 (brown line) for the duration of two pulses. The

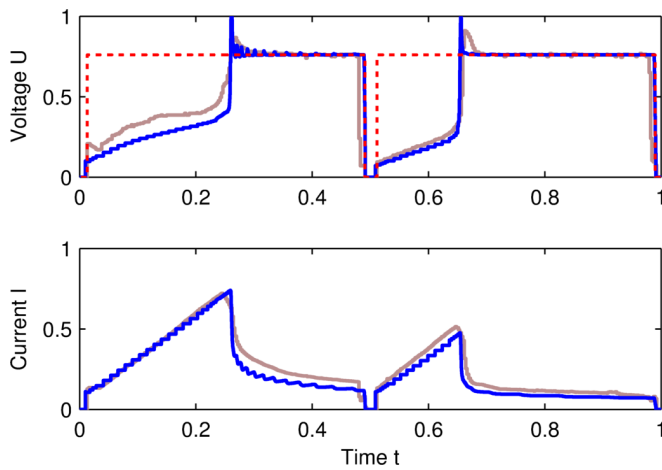


Fig. 4. Normalized characteristic course of the measured (brown), simulated (blue) and desired (dotted red) effective electric voltage and current.

electric variables show a similar behavior during each pulse, which can essentially be divided into two phases. The first phase is characterized by a large deviation between the desired and actual voltage, which is due to a limitation of the rate of the current's increase that is necessary in order to prevent sparking. The beginning of the second phase is marked by a sudden increase of the impedance, after which the imposed voltage closely follows the desired value.

B. Simulation results

The mathematical model was implemented with MATLAB/Simulink. The temperature PDE was discretized using finite differences with a spatial discretization of approximately 0.2 mm. The resulting system of ordinary differential equations consists of 118 state variables was numerically integrated using the ODE solver ODE15S to account for the stiff non-linear dynamics.

The simulated electric variables are in good agreement with the measurements, compare Fig. 4 (blue line). The dynamics during both phases is well reproduced by the simulation model, with only minor deviations from the measured data. The temperature distribution shown in Fig. 5 shows a rapid increase of the temperature close to the edge of the instrument which corresponds well to the evaluation of the surface temperature during similar experiments.

IV. DISCUSSION AND CONCLUSION

In this work, a mathematical model for the analysis of the dynamics of bipolar vessel sealing is proposed. The simulated electric variables and temperature distribution correspond well to measurements of *ex vivo* experiments. The model is able to reproduce the characteristic phases as well as the transition between. While experimental data was limited to the effective voltage imposed to the tissue and the resulting electrical current, the simulation model offers a more detailed insight into the dynamics of the vessel sealing process. The analysis of the spatial distribution of the current density shows that it is comparably homogenous during the first phase, but becomes significantly less homogenous in the

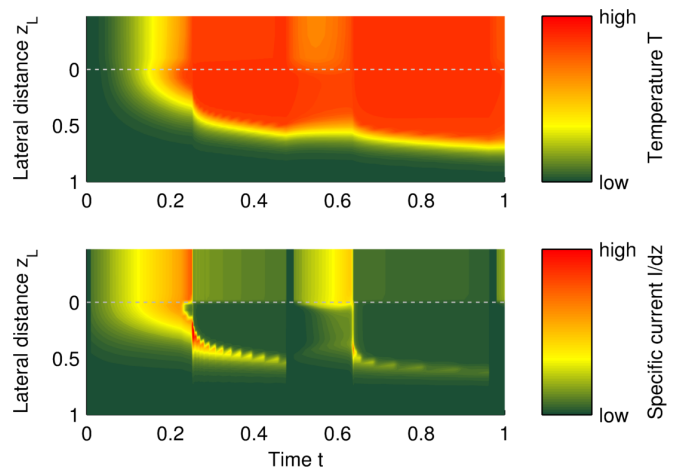


Fig. 5. Normalized spatial distribution of the temperature and the specific current over time. Note that $z_L = z - w_M$. The gray dashed line marks the edge of the electrode.

second phase, see Fig. 5. The electrical current is diverted into the lateral tissue, while the current density in the medial tissue is notably reduced. The extent of the lateral current flow depends on the chosen approximation of the electric field.

The excellent prediction of the electrical and temperature variables make the model suitable for a more detailed analysis of the thermofusion process and to develop and test improved generator strategies. The model may be used to compare the lateral damage of different control strategies and thus help to minimize the thermal damaging of the surrounding tissue. Furthermore, the model may serve for a systematical analysis of the influence and interdependency of different parameters. As a result, simulation studies using the proposed model may be used to improve the experimental setup and key parameters of the bipolar vessel sealing system, further increasing reliability and thus improving the safety of the patient.

REFERENCES

- [1] J. Landman, K. Kerbl, J. Rehman, C. Andreoni, P. A. Humphrey, W. Collyer, E. Olweny, C. Sundaram, and R. V. Clayman, "Evaluation of a vessel sealing system, bipolar electrosurgery, harmonic scalpel, titanium clips, endoscopic gastrointestinal anastomosis vascular staples and sutures for arterial and venous ligation in a porcine model," *The Journal of Urology*, vol. 169, no. 2, pp. 697 – 700, 2003.
- [2] R. E. Dodde, S. F. Miller, J. D. Geiger, and A. J. Shih, "Thermal-electric finite element analysis and experimental validation of bipolar electrosurgical cautery," *Journal of manufacturing science and engineering*, vol. 130, no. 2, pp. 1087–1357, 2008.
- [3] R. Chen, M. Chastagner, R. Dodde, and A. Shih, "Electrosurgical vessel sealing tissue temperature: Experimental measurement and finite element modeling," *Biomedical Engineering, IEEE Transactions on*, vol. 60, no. 2, pp. 453–460, Feb 2013.
- [4] A. Gonzalez-Suarez, J. Alba, M. Trujillo, and E. Berjano, "Experimental and theoretical study of an internally cooled bipolar electrode for rf coagulation of biological tissues," in *Engineering in Medicine and Biology Society, EMBC, 2011 Annual International Conference of the IEEE*, Aug 2011, pp. 6878–6881.
- [5] R. A. Serway and J. W. Jewett, *Physics for Scientists and Engineers with Modern Physic*. Cengage Learning, 2013.
- [6] F. A. Duck, *Physical Properties of Tissues: A Comprehensive Reference Book*. Academic Press, 1990.